

Speed Dependence of Pressure Broadening in Molecular Rotational Spectra Using a Novel Technique

G. Buffa, S. Carocci, A. Di Lieto, P. Minguzzi, F. Quochi, O. Tarrini, and M. Tonelli

Dipartimento di Fisica dell'Università, Piazza Torricelli 2, I-56126 Pisa, Italy

(Received 7 November 1994)

The line shape of a mm-wave rotational transition of CH₃I in an excited vibrational state is observed for molecules in different velocity classes. The collisional self-broadening is measured as a function of relative speed by a novel experimental approach and clear evidence of speed dependence is observed. This result confirms the failure of an oversimplified model, which however is still widely used. We discuss it in detail, and we also show that the rotational temperature of the perturbing molecules has a large influence on the pressure broadening coefficient.

PACS numbers: 33.70.Jg, 33.20.Bx

The broadening effect of collisional relaxation in molecular and atomic spectroscopy has been studied both experimentally and theoretically for many years. Recently, the interest in this field has increased because accurate values of the pressure broadening coefficients γ , and of their temperature dependence, are needed for retrieving the distributions of different compounds from atmospheric spectra. A power law for temperature dependence,

$$\gamma \propto T^{-n}, \quad (1)$$

is commonly assumed.

A different scheme to attack the same problem is to study the dependence of γ on the speed of the colliding molecules, and several recent works were devoted to this approach [1–10], but still some important questions remain open. In this case too a simple power law,

$$\gamma \propto v_r^q, \quad (2)$$

is assumed, where v_r is the relative speed in the collision. Since the average velocity is proportional to $T^{1/2}$, the equation

$$n = 1 - q/2 \quad (3)$$

is used to relate the temperature exponent n to the velocity exponent q . The extra 1 in Eq. (3) is due to the usual practice of expressing γ in units of frequency/pressure. Equations (1) and (2) are practical laws based on elementary theoretical models [11,12]; however, they can be useful when the observed temperature (or velocity) range is not too large.

Velocity studies were devoted either to the distortions that this dependence introduces in the line profile of a gas at thermal equilibrium [mainly in the infrared (IR) and optical regions [5–8]] or to their counterpart in the time domain, namely, the departures from the exponential decay after a pulsed excitation (in the microwave and mm-wave regions [1–4]). Experiments of this kind are extremely difficult because the searched effect is small and can be masked by other causes; therefore, accurate measurements with a high signal-to-noise ratio

are necessary. A more direct investigation of the problem is obtained if single velocity classes can be selectively excited. In the IR region, this was realized by laser saturation measurements in Ref. [9] and by a pulsed technique with Stark switching in Ref. [10]. But even in these cases experiments are not easy because the relevant information is entangled with other effects.

We follow a different approach [13] to excite molecules in selected velocity classes. A cw frequency-stable CO₂ laser is tuned to the $P(8)$ line at 10.5 μm , very close to the IR frequency ν_{IR} of the CH₃I transition from the ground state $J = 9, K = 8$ rotational level, to the vibrational state $\nu_6 = 1, J = 10$, and $Kl = 9$. This excited level is hence populated by laser pumping, and a spectral analysis is performed to measure the profiles of the rotational lines in the mm-wave region, at frequencies near 150 GHz. Here we report results for the hyperfine transition $(\nu_6, J, Kl, F) = (1, 10, 9, \frac{15}{2}) \rightarrow (1, 9, 9, \frac{13}{2})$, but qualitatively similar results were obtained also on other hyperfine components. A schematic diagram of the experimental apparatus is displayed in Fig. 1. The laser frequency is stabilized at the desired value (with a resolution of about 10 kHz) by a frequency-offset-locking technique, using as a reference a second CO₂ laser stabilized by the saturated fluorescence technique. The sample cell is a mm-wave resonator about 90 cm long, which has a hybrid Fabry-Pérot structure with a quality factor $Q \approx 6 \times 10^4$; further details about the microwave circuits can be found in Ref. [14]. To record a line profile, the klystron frequency is scanned, under computer control, while the resonator transmission is detected by a synchronous amplifier tuned to the frequency of the laser chopper [13]. The power transmitted through the sample cell is not absorbed, but it is slightly increased by a process of stimulated emission, because the laser populates the higher of the two rotational levels connected by the transition.

The IR excitation is velocity selective: If the frequency of the pump laser is detuned by an amount $\Delta\nu_{\text{IR}}$ from the exact IR resonance, it can be absorbed only by molecules with a velocity component in the direction of the laser

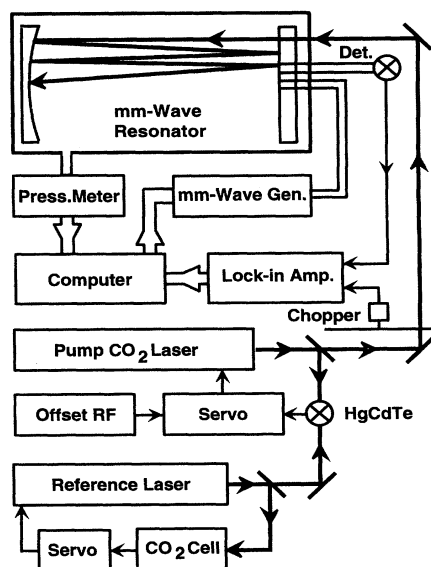


FIG. 1. Schematic diagram of the experimental setup. The mm-wave generator is a phase-locked klystron frequency doubled by a GaAs Schottky-barrier diode. The pressure meter is a high-quality capacitance manometer. The offset radio-frequency generator is used to preset the frequency difference between the lasers. By referencing the amplifier of the mm-wave detector to the frequency (1 kHz) of the laser chopper, only the molecules in the excited vibrational state are observed.

beam given by $v_{e,z} = c\Delta\nu_{\text{IR}}/\nu_{\text{IR}}$. The laser travels inside the sample gas almost collinearly with the mm-wave radiation; therefore, a Doppler shift is induced also on the rotational transitions. Moreover, since both the laser and the mm waves are reflected back and forth by the resonator mirrors, we observe a splitting of the mm-wave lines into two components, which correspond to counter-propagating and copropagating radiations. A single line is observed only when $\Delta\nu_{\text{IR}} \approx 0$, while in other cases two mm-wave lines are present with a frequency displacement $\Delta\nu_{\text{mm}} = \pm\nu_{\text{mm}}\Delta\nu_{\text{IR}}/\nu_{\text{IR}}$. Examples are shown in Fig. 2. The measurement of the splitting allows a direct accurate calibration of the velocity scale; the observed $\Delta\nu_{\text{mm}}$ is consistent at the level of 2% with the preset detuning of the laser, and this puts an upper limit to the effect of velocity changing collisions.

The analysis of the observed raw spectra must take into account the distortion introduced by the mode of the mm-wave resonator. Independent measurements of the cavity transmission are recorded, in the absence of the laser, by an amplitude modulation technique and used to apply suitable corrections to the line shapes. For each value of the laser detuning, the measurements are repeated at several different pressures: the explored range is typically 0.1 to 7 Pa. The analysis of the profiles starts with an estimation of the doublet splitting from recordings at low pressures, then a twin Lorentzian profile at this fixed distance is fitted

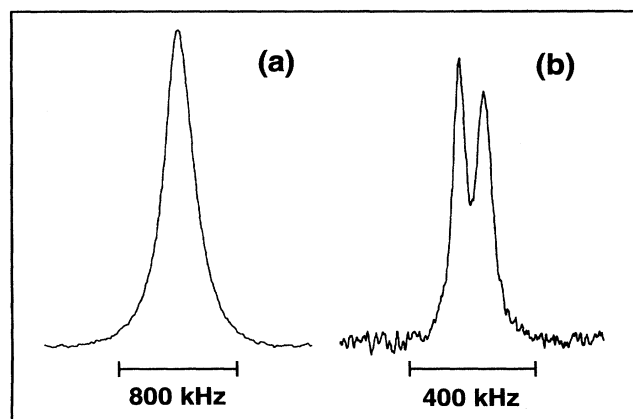


FIG. 2. Examples of recorded line shapes for different pressures and IR detunings: (a) $\Delta\nu_{\text{IR}} \approx 0$, $p = 1.5$ Pa; (b) $\Delta\nu_{\text{IR}} = 7.5$ MHz, $p = 0.15$ Pa. These are raw recordings, not corrected for the (small) distortion caused by the mode of the mm-wave resonator. The pump laser power is about 2 W.

to the data, to evaluate the width of the lines. A Lorentzian shape is an acceptable choice because of the essentially Doppler-free nature of the experiment, and it is consistent with the observed profiles. The widths are subsequently plotted versus pressure, a straight line is fitted to the measurements, and the slope is the experimental estimate of the pressure broadening coefficient γ at the given laser detuning $\Delta\nu_{\text{IR}}$. The same result is obtained if the set of all profiles at a given detuning and different pressures is analyzed simultaneously to yield the estimated slope and splitting. The width extrapolated to zero pressure is typically 15 kHz (HWHM); it can probably be ascribed to wall collisions and other small spurious effects, and it should be compared with the 80 kHz Doppler width at the operating (room) temperature.

Should one expect a dependence of γ on $\Delta\nu_{\text{IR}}$? Because of the velocity selection operated by the laser, our spectroscopic method looks at molecules whose relative velocity in the collisions has not the Maxwell distribution, but the conditional distribution

$$f(v_r|v_{e,z}) = 2 \frac{v_r \sqrt{\alpha}}{v_0^2 \sqrt{\pi}} \exp\left(-\frac{v_r^2}{v_0^2}\right) \times \int_{-v_r}^{v_r} \exp\left[\frac{u^2 - \alpha(v_{e,z} - u)^2}{v_0^2}\right] du, \quad (4)$$

where $v_0 = [2kT(m_e + m_p)/m_e m_p]^{1/2}$ is the most probable relative velocity at thermal equilibrium, m_e and m_p being the masses of the emitting and perturbing molecules, respectively, and $\alpha = 1 + m_e/m_p$. The rms velocity of the conditional distribution in Eq. (4) is $\bar{v}_r = [v_{e,z}^2 + v_0^2(1 + 1/2\alpha)]^{1/2}$, which has to be compared with the value $\bar{v}_r = v_0\sqrt{3/2}$ of the Maxwell distribution. Equation (4) holds for the general case of collisions with a foreign gas, but in our case $m_e = m_p$ and $\alpha = 2$: The shape of

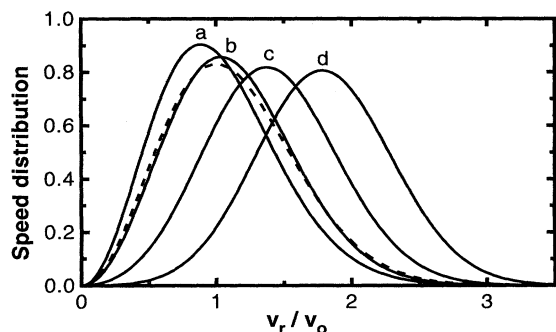


FIG. 3. Conditional relative velocity distribution function $f(v_r | v_{e,z})$ (in the case $m_e = m_p$) for $v_{e,z} = 0$ (a), $v_{e,z} = v_0/2$ (b), $v_{e,z} = v_0$ (c), and $v_{e,z} = 3v_0/2$ (d). The dashed curve is the Maxwellian distribution.

the conditional velocity distribution is displayed in Fig. 3, where it is plotted for different values of $v_{e,z}/v_0$ and compared to the Maxwellian distribution.

On the whole, by changing the IR detuning $\Delta\nu_{\text{IR}}$, we can select particular values of the emitter velocity $v_{e,z}$ in the direction of the laser beam and hence change the average relative velocity \bar{v}_r of the broadening collisions. In Fig. 4 the experimental results are reported and the measured trend with \bar{v}_r (dotted line) is compared to the trend predicted by theory (solid line). Theoretical calculations were performed by the semiclassical approximation of Anderson, Tsao, and Curnutte (ATC) [15] as modified for the case of a hyperfine line [14]. The dipole-dipole, dipole-quadrupole, and quadrupole-quadrupole interactions were considered, using the value $Q = 5.35 \times 10^{-26}$ esu [16] for the molecular electric quadrupole moment of CH_3I , and a numerical integration over the velocity distribution of Eq. (4) was performed. The perfect agreement between experimental and theoretical results is probably somewhat accidental, but the existence of a velocity dependence

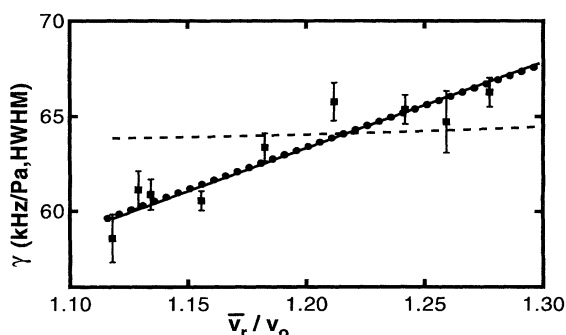


FIG. 4. Pressure broadening coefficient γ versus rms relative velocity. Dotted line is the best fit to experimental results. The solid line is the trend calculated by the ATC approximation. The dashed line is what one would obtain if the rotational temperature of the perturbing molecules would be changed consistently with the rms relative velocity.

of the relaxation rate γ is evident. A fit of Eq. (2) to our experimental results yields $q = 0.84(28)$ at 95% confidence level.

It is common in the literature to relate the value of q to the intermolecular force acting during the collision. For an interaction potential V depending on the distance r as r^{-m} , one should get [6,9–11,17]

$$q = (m - 3)/(m - 1), \quad (5)$$

and hence the expected q values range from 0 ($m = 3$), which is the case of a dipole-dipole potential, to 1 ($m = \infty$), for a hard sphere potential. Since in our case the interaction is mainly dipole-dipole, Eq. (5) is in complete disagreement with experimental results. A similar difficulty was met in Refs. [9] and [10].

As a matter of fact, Eq. (5) is obtained from an oversimplified version of the semiclassical impact approximation and is exceedingly crude for most cases. Better accuracy is obtained if the energy transfer is taken into account, which in the ATC approximation is realized by the so-called resonance functions $f_{\text{int}}(k)$. They give, for each particular interaction, the dependence of the broadening efficacy of a collisional transition on the quantity

$$k = \tau \Delta E / \hbar, \quad (6)$$

where ΔE is the energy transferred to translation from the internal degrees of the colliding pair and τ is the duration of the collision. The resonance functions $f_{\text{int}}(k)$ have different shapes for different interactions, but in every case they rapidly fall off to 0 for large values of k , which by Eq. (6) mean large τ and hence low v_r . As a consequence, q values are obtained larger than predicted by Eq. (5). In fact, also for the case of the dipole-dipole interaction, a velocity dependence of the relaxation rate is expected. Figure 5 shows the result of calculations performed for the presently investigated line, taking into account only the dipole-dipole interaction. The relaxation rate referred to a single perturber $\sigma v_r = \gamma p / N$ is displayed versus v_r . Here σ is the collisional broadening cross section, p the

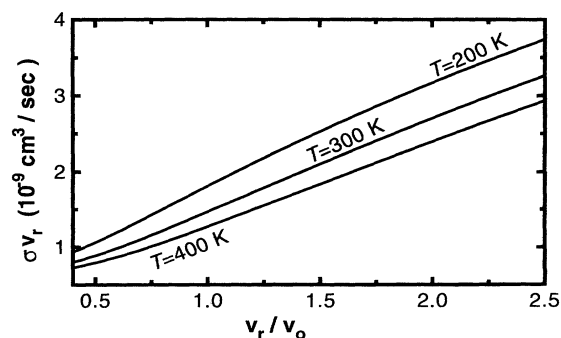


FIG. 5. Calculated dependence of the relaxation rate σv_r on the relative velocity v_r for the dipole-dipole interaction. The relaxation rate depends also on the rotational temperature T of the perturbing molecules.

gas pressure, and N its density. The speed dependence of the relaxation rate is well evident. Moreover, one can also see a marked dependence on the rotational temperature of the perturbing molecules. For this reason different results are obtained if the velocity dependence of γ is studied by velocity selection, as we do, or by temperature variation. The dashed line in Fig. 4 reports the calculation for what one would obtain if the rotational temperature of the colliding molecules would be changed consistently with the rms relative velocity: the v_r dependence of γ would be closer to the constant value predicted by Eq. (5). In fact, the widespread use of Eq. (5) is supported by experiments which measure the temperature dependence of γ , in the case of the dipole-dipole interaction, and find values close to 1 for the exponent n . By Eq. (3) this would mean that q is close to 0. However, this confirmation is misleading because two opposite effects are present: the relaxation rate increases with the relative velocity [smaller τ in Eq. (6)] and decreases with the rotational temperature of the perturber [larger ΔE in Eq. (6)]. This balance is not at all general: an opposite effect of perturber population is expected [18] for lines with a rotational quantum number J larger than the most populated value, $\bar{J} \approx 20$ in our case.

In summary, our investigation leads to three main results. First, the pressure self-broadening of molecular rotational transitions depends on the relative speed of the colliding molecules: While not unexpected on the basis of previous work, the clear evidence of this result comes from a direct and clean experiment with sub-Doppler resolution, backed by a simple theory that carefully and correctly uses the standard ATC approach to deal with these problems. Second, this evidence confirms that the relation in Eq. (5) connecting the speed dependence of the relaxation rate to the distance dependence of the interaction may be completely wrong; for the case of the dipole-dipole interaction it predicts no variation, while an evident variation was found in our measurements. Equation (5) has been criticized in some careful studies, but, as a matter of fact, it is still used by many authors, at least as a rough guide, for comparison with experimental results. Third, the relation in Eq. (3) connecting the speed dependence of the relaxation rate to the temperature dependence of the pressure broadening coefficient is also wrong, if the perturb-

ing particle has low lying energy levels, such as molecular rotational levels.

As a final remark, we note that the experimental approach described here is general and it can be used in other spectral regions, as long as the frequency of the radiation sources is measured accurately.

-
- [1] S.L. Coy, J. Chem. Phys. **73**, 5531 (1980).
 - [2] M.J. Burns and S.L. Coy, J. Chem. Phys. **80**, 3544 (1984).
 - [3] J. Haekel and H. Mäder, J. Quant. Spectrosc. Radiat. Transfer **46**, 21 (1991).
 - [4] F. Rohart, H. Mäder, and H.W. Nicolaisen, J. Chem. Phys. **101**, 6475 (1994). This paper contains an up-to-date review of the problem of speed dependence.
 - [5] S.C.M. Luijendijk, J. Phys. B **10**, 1735 (1977); **10**, 1741 (1977).
 - [6] I. Shannon, M. Harris, D.R. McHugh, and E.L. Lewis, J. Phys. B **19**, 1409 (1986).
 - [7] R.L. Farrow, L.A. Rahn, G.O. Sitz, and J.G. Rosasco, Phys. Rev. Lett. **63**, 746 (1989).
 - [8] J.P. Bouanich, C. Boulet, G. Blanquet, J. Walrand, and D. Lambot, J. Quant. Spectrosc. Radiat. Transfer **46**, 317 (1991).
 - [9] A.T. Mattick, N.A. Kurnit, and A. Javan, Chem. Phys. Lett. **38**, 176 (1976).
 - [10] S.B. Grossman, A. Schenzle, and R.G. Brewer, Phys. Rev. Lett. **38**, 275 (1977).
 - [11] C.H. Townes and A.L. Schawlow, *Microwave Spectroscopy* (Dover, New York, 1955), p. 368.
 - [12] L.D. Landau and E.M. Lifshitz, *Quantum Mechanics* (Pergamon, New York, 1965), p. 488.
 - [13] S. Carocci, P. Minguzzi, F. Neri, and A. Di Lieto, J. Mol. Spectrosc. **163**, 604 (1994).
 - [14] G. Buffa, A. Di Lieto, P. Minguzzi, O. Tarrini, and M. Tonelli, Phys. Rev. A **37**, 3790 (1988).
 - [15] P.W. Anderson, Phys. Rev. **76**, 647 (1949); C.T. Tsao and I. Curnutte, J. Quant. Spectrosc. Radiat. Transfer **2**, 41 (1962).
 - [16] D.L. Vanderhart and W.H. Flygare, Mol. Phys. **18**, 77 (1970).
 - [17] H.M. Pickett, J. Chem. Phys. **73**, 6090 (1980).
 - [18] G. Buffa, O. Tarrini, P. De Natale, M. Inguscio, F.S. Pavone, M. Prevedelli, K.M. Evenson, L.R. Zink, and G.W. Schwaab, Phys. Rev. A **45**, 6443 (1992).